NEODYMIUM PARTITIONING IN ZIRCONOLITE-BASED GLASS-CERAMICS DESIGNED FOR MINOR ACTINIDES IMMOBILIZATION

P. Loiseau, Daniel Caurant, N. Baffier, Catherine Fillet

NEODYMIUM PARTITIONING IN ZIRCONOLITE-BASED GLASS-CERAMICS DESIGNED FOR MINOR ACTINIDES IMMOBILIZATION

P. Loiseau [1], D. Caurant [1], N. Baffier [1] and C. Fillet [2]

1 – Laboratoire de Chimie Appliquée de l'Etat Solide (UMR 7574), ENSCP, 11 rue Pierre et Marie Curie, 75231 Paris Cedex 05, France

2 – Commissariat à l'Energie Atomique (CEA), Centre d'Etudes de la Vallée du Rhône, DCC/DRRV/SCD/LEBM, BP 171, 30207 Bagnols-sur-Cèze, France

Keywords: glass-ceramic, zirconolite, minor actinide conditioning, neodymium partitioning

ABSTRACT

This study deals with glass-ceramic matrices designed for the conditionning of minor actinides, in which zirconolite crystals ($CaZrTi_2O_7$) are homogeneously dispersed in a residual glassy matrix. Good immobilization performances require a high enrichment of actinides in the crystalline phase (double containment principle). Glass-ceramics are obtained by controlled devitrification of an aluminosilicate parent glass containing large amounts of TiO_2 and ZrO_2. Neodymium was selected to simulate the trivalent minor actinides. Crystallization was performed at 1200°C for various Nd_2O_3 contents (0 - 10 wt. %). In all cases, zirconolite crystallization is obtained in the bulk of glass-ceramics. The evolution of Nd^{3+} location between the crystals and the residual glass was followed by electron spin resonance and optical absorption. Both techniques demonstrate that neodymium is partly incorporated in zirconolite crystals. Moreover, total Nd_2O_3 content in parent glass has a strong effect on Nd^{3+} ions distribution.

INTRODUCTION

Current investigations are achieved on new matrices for the specific immobilization of minor actinides that would come from an enhanced reprocessing of nuclear spent fuel. Glass-ceramics containing highly durable crystals accommodating large amounts of actinides, such as zirconolite (**1**), are good candidates. In this case, a high enrichment of actinides in the crystalline phase is required in order to get a double containment of radionuclides in crystals themselves embedded in a durable residual glass. Neodymium was selected to simulate minor trivalent actinides such as Am^{3+} and Cm^{3+} ions because of their similar ionic radii. For instance, in an eight-coordinated site, which is the coordination of the largest site (calcium) of zirconolite, the ionic radii of Nd^{3+} and Am^{3+} ions are respectively 1.109 and 1.09 Å (**2**). Glass-ceramic samples were obtained by controlled devitrification at 1200°C of an aluminosilicate parent glass containing large amounts of TiO_2 and ZrO_2 and various Nd_2O_3 contents (0 - 10 wt. %). Zirconolite is the only phase that crystallizes in the bulk. But a crystallized layer, composed of titanite, anorthite and few baddeleyite crystals, forms at the surface (**3**). This layer whose thickness does not exceed 1 mm was separated from the bulk of glass-ceramics. The results, which are discussed here, focus on the characterization of bulk glass-ceramic by electron spin resonance (ESR) and optical absorption spectroscopies, particularly on the evolution of neodymium partitioning between the zirconolite crystals and the residual glass with total Nd_2O_3 content.

EXPERIMENTAL

Parent glasses with various Nd_2O_3 contents, ranging from 0 to 10 wt. %, were prepared on the basis of the following undoped glass composition (wt. %) (**4,5**):

SiO_2 (43.2), Al_2O_3 (12.7), CaO (20.9), ZrO_2 (9.0), TiO_2 (13.2), Na_2O (1.0)

The compositions of Nd-doped glasses were calculated by keeping the relative proportions of all the other oxides constant. A two-step melting at 1550°C with an intermediate grinding stage was performed to obtain more homogeneous glasses. A 2 h nucleation stage at 810°C followed by a 2 h crystal growth stage at 1200°C led only to the crystallization of zirconolite in the bulk of all the

glass-ceramic samples, irrespective of their neodymium composition. Reference zirconolite ceramics having compositions of $Ca_{1-x}Nd_xZrTi_{2-x}Al_xO_7$ ($0 \leq x \leq 0.6$) were prepared by solid state reaction at 1460°C. A PGT analyzer was used for energy dispersive X-ray (EDX) analysis (accelerating voltage of 15 kV, beam current of about 1.8 nA). Nd^{3+} ion is a paramagnetic and optically active local probe; its electronic configuration and ground state are respectively $4f^3$ and $^4I_{9/2}$. Electron spin resonance (ESR) spectra were recorded on powdered samples (≈ 100mg). Typical measurements were made at 12 K with a microwave power of 20 mW, using a Bruker ESP 300e spectrometer operating at X-band ($\nu \approx 9.5$ GHz) and equipped with a TE_{102} rectangular cavity and an Oxford variable temperature accessory. Optical transmission experiments were carried out at room temperature on KBr pellets (≈ 200mg) containing 25 wt. % of Nd-doped material. Absorption spectra between 424 and 442 nm ($^4I_{9/2} \rightarrow {}^2P_{1/2}$ Nd^{3+} transition) were recorded on a Varian Cary 5E double beam spectrometer. This transition is interesting because the degeneracy of $^2P_{1/2}$ state is not removed by the crystal field. At the most, the $^4I_{9/2}$ ground state is decomposed by the crystal field into five Stark levels which are thermally populated following a Boltzman repartition. So, each type of neodymium site is characterized by a maximum of five lines whose positions depend on the crystal field.

RESULTS AND DISCUSSION

The microstructure of zirconolite crystals formed in glass-ceramics bulk at 1200°C is quite insensitive to neodymium content. These crystals are lath-shaped: their length is around 10 µm and thickness is less than 1 µm (**3,6**). Because of this submicronic thickness, EDX analyses of zirconolite crystals are imprecise, always including a contribution from residual glass. Table 1 reports three examples of EDX results concerning the 0, 6 and 10 wt. % Nd_2O_3 glass-ceramic bulk.

Table 1. Molar compositions determined by EDX for the phases formed at 1200°C in the bulk (residual glass and zirconolite) of glass-ceramics containing 0, 6 and 10 wt. % Nd_2O_3. Molar expected compositions of corresponding parent glasses are indicated in italics.

	SiO_2	Al_2O_3	CaO	TiO_2	ZrO_2	Nd_2O_3	Na_2O
0 wt. % Nd_2O_3							
parent glass	*48.84*	*8.48*	*25.33*	*11.28*	*4.97*	*0.00*	*1.10*
residual glass	54.49	9.43	25.63	7.17	2.23	0.00	1.05
zirconolite	4.52	1.61	24.52	44.26	24.65	0.00	0.44
6 wt. % Nd_2O_3							
parent glass	*48.23*	*8.37*	*25.01*	*11.14*	*4.90*	*1.27*	*1.08*
residual glass	53.68	9.10	25.00	7.39	2.38	1.21	1.24
zirconolite	7.06	3.06	21.79	41.06	24.10	2.29	0.64
10 wt. % Nd_2O_3							
parent glass	*47.77*	*8.29*	*24.77*	*11.04*	*4.86*	*2.20*	*1.07*
residual glass	52.61	8.89	24.72	7.69	2.56	2.09	1.44
zirconolite	8.97	3.72	20.72	39.40	23.27	3.23	0.69

Silicon detection in zirconolite analyses is indicative of residual glass contribution. Indeed, zirconolite is known not to easily incorporate silicon. As a consequence, the following rough estimations of zirconolite composition were deduced after removing residual glass contribution and excluding sodium (very low level): $Ca_{0.97}Zr_{1.07}Ti_{1.90}Al_{0.06}O_7$ for the undoped glass-ceramic, $Ca_{0.82}Nd_{0.19}Zr_{1.05}Ti_{1.77}Al_{0.17}O_7$ for the 6 wt. % Nd_2O_3 and $Ca_{0.76}Nd_{0.26}Zr_{1.04}Ti_{1.74}Al_{0.20}O_{7.01}$ for the 10 wt. % Nd_2O_3 glass-ceramics. This confirms XRD results (**7**) which showed that neodymium incorporation inside zirconolite crystals increases without saturation effect when Nd_2O_3 total wt. % ranges from 0 to 10 %. Moreover, these results indicate that neodymium is essentially incorporated in the calcium site of zirconolite structure with a charge compensation mainly ensured by a partial substitution of titanium by aluminum ions. Nevertheless, for the 10 wt % Nd_2O_3 glass-ceramic, it seems that a part of neodymium (around 0.06 ions by formula unit) is not compensated by aluminum: these Nd^{3+} ions are likely to equally occupy the calcium and zirconium sites of zirconolite structure, which maintains electroneutrality. On the other hand, it can be noticed that an important part of Nd^{3+} ions remains unfortunately in the residual glass. This is mainly due to the

low degree of crystallization of these glass-ceramics (less than 13 % in volume). Because of the difficulty to precisely evaluate the zirconolite composition and especially the degree of crystallization, indirect spectroscopic methods were used to estimate the molar ratio R of neodymium incorporated in the zirconolite crystals versus total neodymium content in the glass-ceramics (**7**). Figure 1 shows typical ESR and optical absorption spectra obtained for parent glass, glass-ceramic bulk and zirconolite ceramic.

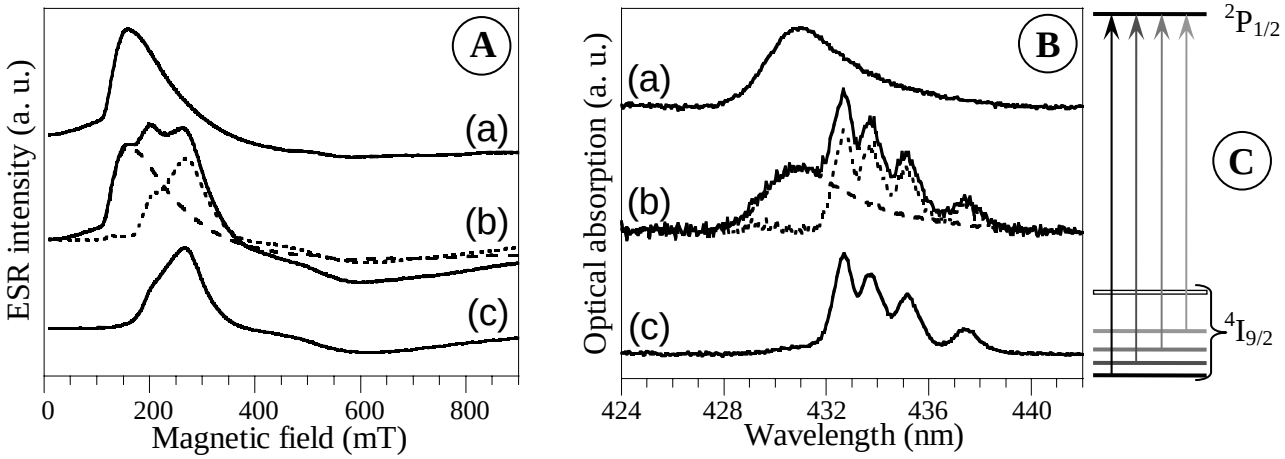

Figure 1. Electron spin resonance (A) and optical absorption (B) spectra of (a) 2 wt. % Nd_2O_3 parent glass, (b) glass-ceramic bulk (continuous-line curves), and (c) $Ca_{0.8}Nd_{0.2}ZrTi_{1.8}Al_{0.2}O_7$ zirconolite ceramic. (C) : schematic neodymium energy levels involved in $^4I_{9/2} \rightarrow {}^2P_{1/2}$ optical transitions for zirconolite.

The differences observed in the ESR and absorption spectra of the three host matrices correspond to different local neodymium environments. The large inhomogeneous broadening (absence of resolution) of the optical transition lines in the glass absorption spectra (Figure 1Ba) is due to a distribution of neodymium environments in accordance with the amorphous nature of the matrix. The optical absorption of Nd-doped zirconolite (Figure 1Bc) exhibits only four lines because the fifth stark level of $^4I_{9/2}$ state is located at too high energy to be thermally populated at room temperature (Figure 1C). Glass-ceramic bulk spectra (ESR and optical absorption) can be decomposed into the contributions of residual glass and zirconolite crystals, as shown in Figures 1Ab and 1Bb. To perform this decomposition, the residual glass signal was assimilated in both cases to the parent glass one (Figures 1Aa and 1Ba), and was subtracted from the glass-ceramic bulk spectrum (Figures 1Ab and 1Bb). The remaining spectra (finely dotted curves in Figures 1Ab and 1Bb) are very close to the ones recorded for the Nd-doped zirconolite ceramic (Figures 1Ac and 1Bc). This analogy indicates that neodymium environments are similar in zirconolite crystals prepared either by devitrification at 1200°C or by solid state reaction at 1460°C. R is first estimated from ESR glass-ceramics bulk spectra (Figure 1Bb), as follows. The double integration of Nd^{3+} ESR signals in zirconolite crystals and in the whole of glass-ceramics (residual glass + crystals) are calculated; their ratio is equal to R. In the case of optical spectra, the determination of R is not as straightforward. Actually, the areas under zirconolite and residual glass optical absorption signals are not only proportional to Nd^{3+} content, but also to oscillator strength of the $^4I_{9/2} \rightarrow {}^2P_{1/2}$ transition (transition probability). Comparison of optical absorption with ESR results allows the evaluation of the neodymium oscillator strengths ratio between the two phases (zirconolite / residual glass), giving access to a further optical estimation of R. Figure 2A shows the variation of R with Nd_2O_3 total content. ESR and absorption results are in total agreement: R decreases with increasing Nd_2O_3 total content. If the degree of crystallization in volume is assumed to be the same irrespective of total Nd_2O_3 content, such a decrease in R would thus indicate that the neodymium concentration increases more slowly in the zirconolite crystals than in the residual glass with increasing total neodymium concentration (0 – 10 wt. %). This would amount to a non-linear dependence of neodymium concentration in zirconolite (which is proportional to the number x of Nd^{3+} ions per zirconolite unit formula) with total neodymium content in glass-ceramics. As x was not measured by EDX for all glass-ceramic compositions, it was calculated from R results. To perform this

calculation, the degree of crystallization in volume was assumed to be constant and the x values determined by EDX for the 6 and 10 wt. % Nd_2O_3 glass-ceramics were coupled to the corresponding R estimations (Figure 2B). Thus, it can be seen that neodymium concentration in zirconolite crystals increases slower when the Nd_2O_3 total level is higher. At least one hypothesis can be put forward to explain this evolution. x may depend on a thermodynamic equilibrium governing neodymium incorporation between the crystalline phase (zirconolite) and the surrounding supercooled liquid (becoming residual glass after quenching). Then, x evolution could be explained by a variation of neodymium activity coefficients (at least in zirconolite, which is the most Nd-concentrated phase) with increasing Nd_2O_3 total content (departure from a Henry's type law expected for diluted concentration, for example).

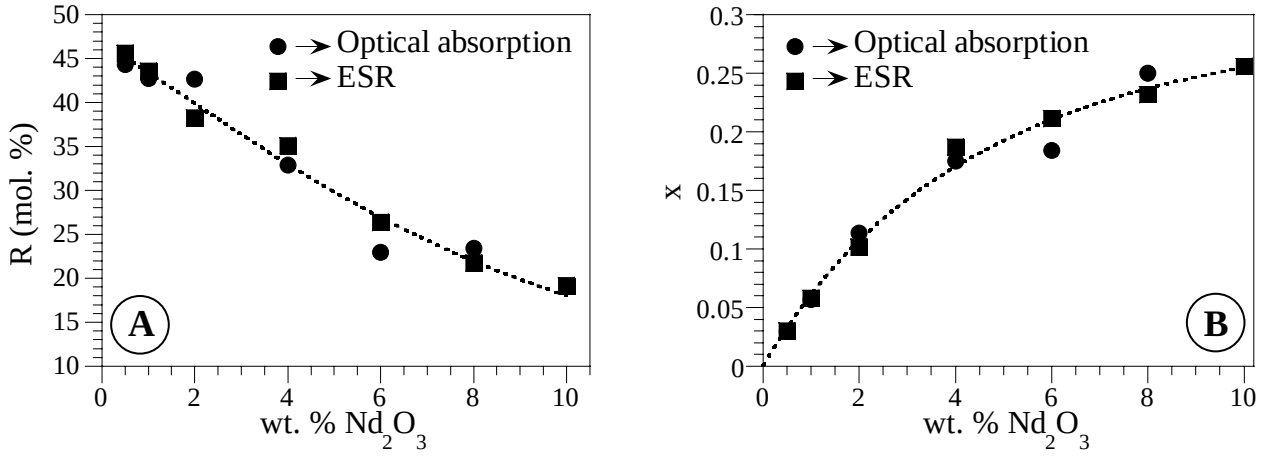

Figure 2. Evolution with Nd_2O_3 total content of: (A) R estimated from ESR and optical absorption spectra of glass-ceramic bulk, (B) number x of Nd^{3+} ions per zirconolite unit formula deduced from R.

CONCLUSION

Zirconolite-based glass-ceramics were obtained at 1200°C. Various Nd_2O_3 contents (0 - 10 wt. %) were investigated as simulant of trivalent minor actinides. It was found that the ratio R (number of Nd^{3+} ions incorporated in zirconolite crystals divided by Nd^{3+} total content) decreases with increasing Nd_2O_3 total content. This evolution would be mainly due to a non-linear dependence of x (number of Nd^{3+} ions per zirconolite unit formula) versus Nd_2O_3 total content. Nevertheless, x is a growing function of Nd_2O_3 concentration in parent glass composition. Complementary EDX analyses are in progress to confirm the estimations of x made from the R results. Moreover, the use of other simulants (europium, gadolinium, thorium) is under study.

REFERENCES

(1) A. E. Ringwood, S. E. Kesson, K. D. Reeve, D. M. Levins, E. J. Ramm, in Radioactive waste forms for the future (eds W. Lutze and R. C. Ewing, Elsevier Science Publishers B. V.) (1988), p. 233

(2) R. D. Shannon, Acta Crystallogr. Sect. **A 32**, 751 (1976)

(3) P. Loiseau, D. Caurant, N. Baffier, L. Mazerolles, C. Fillet, Scientific Basis for Nuclear Waste Management XXIV, Mat. Res. Soc. Symp. Proc. (2000)

(4) C. Fillet, J. Marillet, J. L. Dussossoy, F. Pacaud, N. Facquet-Francillon, J. Phalippou, Environmental Issues and Waste Management Technologies in the Ceramic and Nuclear Industries III, **87**, 531 (1997)

(5) T. Advocat, C. Fillet, J. Marillet, G. Leturcq, J. M. Boubals, A. Bonnetier, Scientific Basis for Nuclear Waste Management XXI,. Mat. Res. Soc. Symp Proc., 55 (1998)

(6) P. Loiseau, D. Caurant, I. Touet, Y. Dextre, C. Fillet, Atalante 2000 (this issue)

(7) P. Loiseau, D. Caurant, N. Baffier, C. Fillet, Scientific Basis for Nuclear Waste Management XXIV, Mat. Res. Soc. Symp. Proc. (2000)